*Journal of Statistical Physics, Vol. 60, Nos. 1/2, 1990*

# Hypercube Stacking: A Potts-Spin Model for Surface Growth

**Bruce M. Forrest**[1,2] **and Lei-Han Tang**[1,3]

*Received December 15, 1989*

We present a deposition and evaporation model for surface growth under a solid-on-solid constraint. We generalize the Ising-spin representation of a two-dimensional surface by Blöte and Hilhorst to a $d$-dimensional surface of a $(d+1)$-dimensional hypercubic lattice. The allowed surface configurations correspond to the (degenerate) ground states of a chiral $d$-state Potts model. We describe a vectorized multisite-coding implementation for the corresponding kinetic Potts-spin model for $d=2$ and $d=3$. For the $d=2$ equilibrium surface our simulation results show excellent agreement with an exact analysis.

**KEY WORDS:** Surface growth; Potts model; solid-on-solid constraint; multisite coding; vectorization.

## 1. INTRODUCTION

The simulation of models exhibiting critical phenomena invariably demands large system sizes in order to determine the proper finite-size scaling forms and extract the correct behavior in the thermodynamic limit. This is of particular importance in growth models where one is interested in the behavior of a surface growing in the presence of stochastic noise of various origins and wishes to characterize its degree of roughness by investigating possible scaling relations of the height fluctuations and correlations within the surface. This can be studied quantitavely by monitoring the development of the width $w(L, t)$ (root-mean-square) of the

[1] Institut für Festkörperforschung, Forschungszentrum Jülich, D-5170 Jülich, Federal Republic of Germany.

[2] Present address: Institut für Theoretische Physik, Universität Heidelberg, D-6900 Heidelberg, Federal Republic of Germany.

[3] Present address: Fakultät für Physik und Astronomie der Ruhr Universität, D-4630 Bochum, Federal Republic of Germany.



0022-4715/90/0700-0181$06.00/0 

height fluctuations of a surface grown over a $d$-dimensional substrate of linear size $L$, where one normally begins with a flat surface at time $t = 0$.

Among the models which have been studied in an attempt to understand surface roughening phenomena are diffusion-limited aggregation[1] (DLA), Eden growth,[2] ballistic deposition,[3,4] and the single-step model.[5,6] The latter three types are simpler than DLA in the sense that they form compact clusters (their fractal dimension being equal to their Euclidean dimension, unlike DLA). Despite the simplicity of the growth mechanisms involved, specifying the surface behavior has proven to be a far from trivial problem. However, it has emerged from simulations of such models that the width is observed to obey a scaling form[3,7]

$$w(L, t) \sim L^{\zeta} f(t/L^{z}) \tag{1}$$

where $f(x) \to \text{const}$ as $x \to \infty$, and $f(x) \propto x^{\zeta/z}$ for $x \ll 0$. The former limit corresponds to the equilibrium width [implying $w(t \gg L^{z}) \sim L^{\zeta}$], while the latter has $w(t \ll L^{z}) \sim t^{\zeta/z}$, so that for small enough times $t$ the surface does not "feel" the finite extent of the underlying substrate. Complementary to numerical investigations, further interest in these models was stimulated by the analytical work of Kardar *et al.*,[8] who carried out a renormalization-group study of a nonlinear Langevin equation proposed to govern a universality class encompassing these growth models. Their analysis suggested that $d_c = 2$ is the upper critical dimension of the substrate, above which there may be a nonequilibrium roughening transition between regimes of weak and strong noise, implying two different scaling regions: one of weak coupling with mean-field exponent $\zeta = 0$, and one of strong coupling possessing a nontrivial roughness exponent $\zeta > 0$.

Accurate determination of the dynamic exponent $\beta = \zeta/z$ is hampered by a number of factors. In growth from a flat surface one typically has an initial period of random deposition before entering the "true" growth regime with $w \sim t^{\beta}$. In order that this growth period may be observed over a reasonable time range, the system size $L$ must be large enough, since $w(L, t)$ will begin to level off for times approaching $t \sim O(L^{z})$ before finally attaining its equilibrium value. Thus, we require $1 \ll w \ll L^{\zeta}$. Moreover, in some of our simulations, determination of $\beta$ was further exacerbated by a slow crossover from transient growth with a smaller exponent to the asymptotic rate. This observation was only made possible due to the large system sizes which we were able to reach.

Determination of the roughening exponent $\zeta$ is also a formidable task, as it involves ensuring that the growth has proceeded long enough to guarantee that the equilibrium width $w(t \gg L^{z})$ is indeed being observed.

Thus, it is clear that in order to accurately investigate such models, we must deal with systems of sufficient size and we must be able to simulate

them over a reasonable length of time. This is, of course, demanding on both computer memory and on cpu time. We present here a model and its numerical implementation which is extremely efficient in both of these respects. The model, which shall be described in the following section, is a deposition and evaporation model consisting of stacking $(d+1)$-dimensional hypercubes above a $d$-dimensional substrate. It can be viewed as a variant of the single-step model of Plischke *et al.*[6] (with the $d=1$ case exactly coinciding with their model) and as such it can be very efficiently coded: it is only necessary to store the evolving surface—unlike, e.g., the Eden model, where, due to the presence of holes and overhangs, one typically needs to store additional sites in the cluster and to have a separate list of surface sites. Furthermore, simple Potts variables ($d$-state in $d$ dimensions) can be introduced, so that the whole model lends itself ideally to multisite coding techniques. This obviously enhances the size of the systems which can be dealt with in a given amount of computer memory and provides a substantial speedup factor, as all of the sites stored in a given computer word are updated simultaneously. We are not aware of any previous *full* multisite-coded implementation of such growth models (previous efforts were at most only partly multisite coded, storing the lattice occupancy as single-bit variables). In addition, our algorithm is vectorizable and the combination of these two features provides a very powerful simulation tool on vector processors such as the Cray. Previous numerical work could only use partially vectorizable code for the simulation of a single cluster. For example, Zabolitzky and Stauffer[9] were able to vectorize their Eden model simulations, but at the expense of a systematic error which decreased with increasing perimeter size of the cluster. To our knowledge, it has not yet been possible in growth model simulations to combine single-bit handling with vectorization in a relatively straightforward manner. We were able to study significantly large system sizes: up to substrate sizes $N=L^2=11520^2$ sites for $d=2$; and $N=2L^3=2\times 192^3$ for $d=3$. (Among all growth model simulations, the only systems of a comparable size were those studied by Zabolitzky and Stauffer,[9] who reached $8192^2$ and $256^3$ in their Eden model simulations on a Cray-2, a computer with 16 times more memory than the one at our disposal, a Cray X-MP/416.)

Our "hypercube-stacking" model, like other models under a solid-on-solid (SOS) restriction, enjoys the further advantage of a comparatively trivial "intrinsic width" (a quantity describing the behavior of the surface on short length scales[10]). This is in contrast to the situation in the Eden model, where holes and overhangs make it difficult and even ambiguous to define a single-valued height. The latter behavior often produces a large correction to scaling,[10,11] complicating the ensuing analysis.

In the next section we describe the model for $d=2$ dimensions and its multisite-coding implementation. We then proceed to show how the model may be generalized to higher values of $d$, giving $d=3$ as a further example, which we also have studied. Some details of the coding for this case are also provided. A test run of the $d=2$ code against an exact result is given. Detailed results of our growth simulations and their analysis shall be presented elsewhere.[12]

## 2. THE TWO-DIMENSIONAL MODEL

We consider the growth of a simple-cubic (SC) crystal growing above a (111) substrate plane as occupation of the SC lattice sites by atoms. A solid-on-solid (SOS) constraint on the surface atoms is always imposed: we define a surface atom as one having (strictly) less than six nearest neighbors and demand that each such surface atom occupies a corner of a *completed* cube (eight occupied corners), which has at most half (three out of six) of its faces exposed. A face of a cube is *exposed* if it is not shared by two completed cubes.

For the purpose of illustration, a similar SOS condition on an analogous situation of a two-dimensional (2D) square-lattice crystal is depicted in Fig. 1. The crystal consists of the black circles and its surface satisfies the SOS condition along the (11) direction (the vertical direction in the figure). Occupation of site $A$ (shown by a white circle) in the crystal at this time would violate the SOS constraint, as it would not correspond to the completion of a new square. Occupation of sites $B$ and $C$ would result in a completed square, but is forbidden since this square would have three "faces" exposed—more than half of its (four) faces. Likewise the four sites $D$, $E$, $F$, and $G$ cannot be occupied, despite forming a completed square, as four—more than half—of its faces would be exposed.

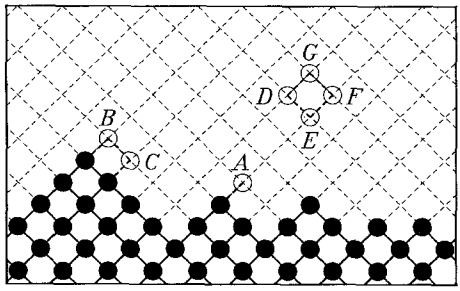


Fig. 1. Example of a two-dimensional square-lattice crystal (the black circles) obeying a solid-on-solid (SOS) restriction along the (11) direction. The sites denoted by open circles would violate the SOS condition if occupied at this time.

This 2D crystal under the SOS constraint can be viewed as a stack of squares on (11) substrate line. Similarly, we can view the three-dimensional (3D) SC crystal considered here as a stack of cubes on the (111) substrate plane. It is also evident that the surface of the SC crystal consists of a singly-connected piece made up of three types of cube faces: namely, squares oriented normal to the (100), (010), and (001) directions, as shown in Fig. 2a. Projection of the surface atoms onto the (111) substrate plane will always give rise to a 2D triangular lattice. Figure 2b shows such a projection of the surface configuration of Fig. 2a. The sites of the 2D triangular lattice are given by the vertices of the rhombic tiles in Fig. 2b, with each rhombus corresponding to the projection of a square on the surface of the crystal (i.e., of an exposed face of a cube on the stack). The three unit vectors $\hat{\mathbf{e}}_1 = (100)$, $\hat{\mathbf{e}}_2 = (010)$, and $\hat{\mathbf{e}}_3 = (001)$ are mapped under this projection onto three vectors $\hat{\mathbf{e}}_\alpha^{\parallel}$, $\alpha = 1, 2, 3$, lying at 60° to one another. Two of these vectors can be taken as basis vectors for the triangular lattice.

We measure height along the (111) direction, so that a surface point having coordinate $\mathbf{R} = \sum_{\alpha=1}^{3} n_\alpha \hat{\mathbf{e}}_\alpha$ will have a height above the (111) substrate plane given by the integer function

$$h(\mathbf{x}) = \sum_{\alpha=1}^{3} n_\alpha \tag{2}$$

where the projection of $\mathbf{R}$ onto the substrate is given by $\mathbf{x} = \sum_{\alpha=1}^{3} n_\alpha \hat{\mathbf{e}}_\alpha^{\parallel}$. It should be clear that the SOS restriction renders the height a single-valued function of position $\mathbf{x}$ in the substrate plane.

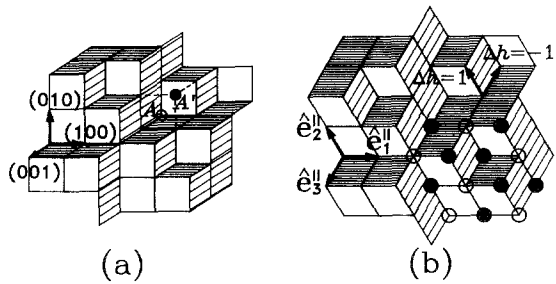


Fig. 2. (a) A cube stack obeying an SOS condition along the (111) direction: only (001), (010), and (100) faces of the cubes may be exposed. Growth at an eligible site such as $A$ corresponds to the addition of an atom at site $A'$, resulting in the addition of a new cube onto the stack. (b) The rhombic tiling obtained by projecting the cube stack onto a (111) substrate plane. The entire surface configuration can be represented by two-state Potts variables (open and closed circles) residing on the vertices of the underlying two-dimensional triangular lattice. A rhombus edge indicates a satisfied antiferromagnetic bond between two neighboring sites. Two sites connected by such a bond have a relative height difference of $\Delta h = \pm 1$.

Note that under the above projection, *all* of the sites of the SC crystal will collapse onto the 2D triangular lattice, but since there will always be a one-to-one correspondence between the surface sites of the crystal and the vertices of the triangular lattice, we may deal exclusively with the projected surface sites, and in that respect sites of the SC crystal not belonging to the surface play no further role on the projected lattice.

As can be seen from Fig. 2, the tiling configuration of rhombi directly reflects relative surface heights. Two neighboring sites on the 2D substrate lattice (Fig. 2b) connected by the edge of a rhombus indicates a height difference of one unit between the sites. Absence of such a rhombic edge between two neighboring sites implies a height difference of two units. That only these two possibilities exist between any pair of neighboring sites on the 2D lattice is a direct consequence of the SOS restriction. To be more precise, let $\mathbf{x}_i$ and $\mathbf{x}_j$ be any two such neighboring sites of the 2D lattice, which are thus related by $\mathbf{x}_i - \mathbf{x}_j = a\hat{\mathbf{e}}_\alpha^{\parallel}$ for some $\alpha \in \{1, 2, 3\}$ and $a = 1$ or $-1$. Then, for $a = 1$ (a case which we shall henceforth refer to as $i$ being a "principal" neighbor of $j$), the height difference $\Delta h_{ij} = h(\mathbf{x}_i) - h(\mathbf{x}_j)$ may only be 1 or $-2$, while for $a = -1$ ($i$ is a "nonprincipal" neighbor of $j$), $\Delta h_{ij} = -1$ or 2 only. The case $|\Delta h_{ij}| = 1$ in fact indicates that on the original surface, sites $i$ and $j$ were nearest neighbors and thus were connected, while $|\Delta h_{ij}| = 2$ indicates that they were not.

In the growth algorithm considered here, we demand that the SOS condition be dynamically preserved. Thus, deposition of an atom at a surface site is possible only if it corresponds to the addition of a new cube onto the existing stack. All but the last vertex of this cube are sites on the original surface, and precisely 3 of the 6 faces of the cube must make contact with the stack. This process can be understood with the help of Fig. 2a. Site $A$ represents a surface site onto which a new atom can be placed at $A'$, thereby adding a new cube to the stack. The new surface site $A'$ has the same projection onto the (111) substrate plane as that of site $A$, but its height is 3 units higher. The reverse process of evaporation ($A' \to A$) is possible only if it corresponds to the removal of a cube which has precisely three exposed faces. This decreases the surface height at the corresponding substrate lattice site by 3 units. The growth velocity of the surface is controlled by two rates: $p^+$ for deposition (addition of a cube) and $p^-$ for evaporation (removal of a cube).

Every stacking event (growth or evaporation at a site on the stack's surface) must maintain the SOS requirement and this means that the number of exposed faces on the stack will always be conserved: an added cube must cover (make contact with) three exposed faces of the stack, but at the same time its three remaining faces will be exposed; on the other hand, a cube which is removed can only be one with three exposed faces, and once

it has been removed, the three faces with which it made contact in the stack will be exposed. Hence, on the projected 2D triangular lattice, the number of rhombi will always be conserved.

In the following we discuss a two-state Potts spin representation (i.e., a spin-1/2 Ising model) of the surface configurations and the growth rules which render a multisite-coding algorithm possible.

As has already been noted by Blöte and Hilhorst,[13] any rhombic tiling (or "diamond covering") of the lattice can be represented as a ground state of the 2D triangular antiferromagnet: the edges of the rhombi correspond to a satisfied (antiferromagnetic) bond between the two connected sites, while the absence of an edge between two neighboring vertices indicates that there is a frustrated bond between those sites. Thus, we can introduce two-state Potts variables $\sigma(\mathbf{x}_i)=0$ or 1 at each vertex $\mathbf{x}_i$ of the lattice such that for any pair of neighbors $(\mathbf{x}_i, \mathbf{x}_j)$, $\sigma(\mathbf{x}_i)\neq\sigma(\mathbf{x}_j)$ signifies a satisfied bond between $\mathbf{x}_i$ and $\mathbf{x}_j$, and $\sigma(\mathbf{x}_i)=\sigma(\mathbf{x}_j)$ indicates a frustrated bond. The lower right-hand part of Fig. 2b shows the Potts variables (open and closed circles) corresponding to the projected surface configuration of Fig. 2a.

Using this representation, the height difference between two neighboring substrate sites can be expressed as

$$\Delta h \equiv h(\mathbf{x}_i+\hat{\mathbf{e}}_\alpha^{\parallel})-h(\mathbf{x}_i)=1-3\delta\{\sigma(\mathbf{x}_i),\sigma(\mathbf{x}_i+\hat{\mathbf{e}}_\alpha^{\parallel})\} \tag{3}$$

where $\delta\{x, y\}=1$ if $x=y$ and 0 otherwise.

To see that the above scheme can be carried out self-consistently, we consider the explicit mapping

$$\sigma(\mathbf{x}_i)=h(\mathbf{x}_i) \bmod 2 \tag{4}$$

That (3) and (4) are consistent can be seen by considering two neighboring sites $\mathbf{x}_i$ and $\mathbf{x}_j\equiv\mathbf{x}_i+\hat{\mathbf{e}}_\alpha^{\parallel}$ on the 2D lattice. Their relative height difference may only be $\Delta h\equiv h(\mathbf{x}_j)-h(\mathbf{x}_i)=1$ or $-2$. If $\Delta h=1$, then $\sigma(\mathbf{x}_i)\neq\sigma(\mathbf{x}_j)$, while if $\Delta h=-2$, then $\sigma(\mathbf{x}_i)=\sigma(\mathbf{x}_j)$, in agreement with (3).

There is a special constraint on $\{\sigma\}$ which corresponds to a single-valued height function. Around any elementary triangular plaquette of the lattice (which is formed by taking each of the three principal vectors $\mathbf{e}_\alpha^{\parallel}$ as its sides) there must be precisely two satisfied bonds and one frustrated bond, since, of course, we must have no net height change on returning around the loop (as indeed must be the case on returning around any loop on the lattice). That is, we must have $\Delta h=+1$ occurring twice and $\Delta h=-2$ once (assuming, without loss of generality, that we traverse the plaquette clockwise, following the $\hat{\mathbf{e}}_\alpha^{\parallel}$). In terms of the Potts variables, out of the three vertices on the plaquette, there must be two of one kind and

one of the other. This constraint of precisely one frustrated bond around any elementary plaquette is equivalent to the statement that any valid Potts configuration for this model must be an antiferromagnetic ground state.

We now describe the kinetic growth rule in terms of the Potts variables. We have already seen above that in order to preserve the SOS condition during growth, only surface sites (i.e., corners of the cubes) which are connected to other surface sites of a higher height may grow, and that growth then corresponds to the addition of a cube onto the 3D stack. This condition for a site to be eligible for growth translates to the 2D lattice as follows. Between the site in question and each of its three principal neighbors there must be a satisfied bond, as a frustrated one would imply a height *decrease* of 2 on going from the site to its neighbor. Similarly, between the site and its other three (nonprincipal) neighbors there can be no satisfied bond, as that would indicate a height *decrease* of 1. Thus, a site is eligible for growth if and only if it has the same spin as all of its three nonprincipal neighbors and has a spin opposite to those of its three principal neighbors. Due to the constraint around any triangular plaquette that we must have two spins of the same type and one of the other type, it is in fact sufficient to check that the three nonprincipal neighbors have the same spin as the central site, for if this is the case, then the three principal neighbors must have the opposite type of spin.

Growth at the eligible site is then simply achieved by flipping the spin $\sigma_i \to 1 - \sigma_i$, as then the height at that site will change from being two less that its three nonprincipal neighbors (and one less than its three principal neighbors) to being one more (and two more than the principal neighbors). Hence the height change will be $\Delta h = 3$. This growth of a site is indicated in Fig. 3 in the left to right direction (with the three nonprincipal neighbors being denoted by open circles). Evaporation is simply the reverse of this procedure: we must check that a site has a spin identical to all of its principal neighbors, and if so, it is then flipped, producing a height decrease of 3 (right to left in Fig. 3).

Thus, using this mapping onto a 2D triangular lattice, only the surface of the crystal need be stored, and furthermore, the state of each vertex of

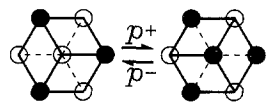


Fig. 3. The local updating procedure for the central site on the two-dimensional triangular lattice. Potts variables are denoted by open ($\sigma = 0$) and closed ($\sigma = 1$) circles. Heavy lines denote satisfied bonds, dashed lines denote frustrated bonds. Deposition takes place at a rate $p^+$ going from left to right. Evaporation, at a rate $p^-$, is in the opposite direction.

this 2D representation, being a two-state Potts variable, only requires one bit of information. This is in sharp contrast to the perhaps more straightforward projection of the 3D crystal down the, say, (001) direction. It would still be possible to employ a spin representation on the projected lattice if a restricted SOS constraint were imposed,[14] i.e., if relative surface heights between neighboring points were restricted to being within some range 0, 1,..., $M$. The spins would, however, have to reside on the interstitial *bonds* and, furthermore, each such spin would require $2M+1$ possible values (as both negative and positive height changes must be accounted for). For the case of the SC crystal here, the projected lattice would be a square lattice, and with two bonds per surface site, this would give rise to $(2M+1)^2$ possible states per surface site. In addition, growth at a single site would involve updating the state of all bonds connected to that site.

We shall see below that this description employing Potts variables residing on the lattice vertices and producing satisfied and frustrated antiferromagnetic bonds has an obvious and useful generalization to higher dimensions. As the coordination number of a hypercubic lattice increases linearly with dimension, the advantage of our model over the straightforward approach is even greater in higher dimensions as far as multisite coding is concerned.

## 3. MULTISITE CODING OF THE 2D MODEL

There is obvious scope for parallelism in the model described above, as the lattice may be subdivided into three sublattices (as shown in Fig. 4) in such a way that the updating of any site on a given sublattice only requires knowledge of sites residing on one of the other two sublattices.

In fact, these three sublattices have a natural interpretation with respect to the original surface: for each sublattice $s$ ($= 1$, 2, or 3) the height

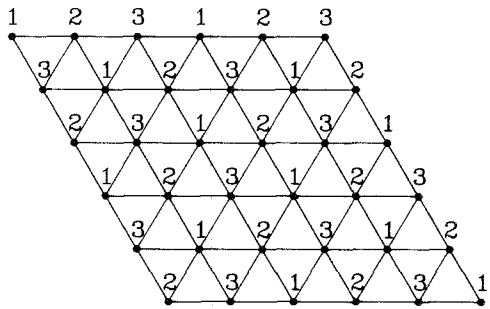


Fig. 4. The natural sublattice structure of the two-dimensional substrate lattice. To update any site on, e.g., sublattice 1, only sites of sublattice 3 need be consulted in the case of deposition, while for evaporation, only sites on sublattice 2 are required.

of any site is of the form $h_i^{(s)} = 3n + s$ for some integer $n$. This follows first from the fact that between any site $i$ and any of its six neighbors $j$, $\Delta h_{ij} = \pm 1$ or $\pm 2$ only. Second, any path between two sites on the same sublattice can be broken down into pairs of successive steps along a principal vector and against a principal vector—such a double step can only result in a height change of $-3, 0$, or 3. It is obvious that the dynamics preserve this property, too, since the growth (evaporation) of a site results in a height change of 3 $(-3)$ at that site.

This subdivision together with the single-bit variables at each vertex makes the simulation of this system ideally suited to a multisite coding[15] implementation—a technique which has already proved to be powerful in other applications both in terms of speed and in efficient use of computer memory.

With regard to the deposition rate $p^+$ (and equivalently, the evaporation rate $p^-$), we could not, of course, implement the deterministic version $p^+ = 1$ while utilizing such a sublattice updating scheme whereby all of the sites on a given sublattice are updated simultaneously: this would ignore completely the stochastic nature of the problem. In particular, an initially flat surface, such as the one employed in our simulations (see below), would remain indefinitely flat for $p^+ = 1$. However, choosing a $p^+$ less than one (and not too close to it) should suffice to avoid such problematic situations arising. For reasons of speed, we chose $p^+ = 1/2$, as will be explained in more detail below, so that on average half of the sites in a given sublattice were allowed to grow. In Section 5 we present results of our simulations, which are in excellent agreement with exact results and we take this as confirmation of the validity of these assumptions.

We simulated a rhombic system of size $L \times L$ with periodic boundary conditions. Our initial configuration corresponded to a flat surface, as shown in Fig. 5. This has an average orientation along the (111) direction and with periodic boundary conditions this required the system size $L$ to be a multiple of 3. In view of this and in order that we might also deal with smaller system sizes, the Fortran implementation of the multisite coding allowed for a variable number $N_B$ of sites stored in each integer, each two-state Potts variable (spin) requiring only one bit of storage—that is, $N_B$ was not necessarily as large as the number of bits in a computer word, so on the Cray, for instance, $N_B \leqslant 64$. Thus, each row of $L$ lattice sites could be accommodated in $M \equiv L/N_B$ integers IS(1), IS(2),..., IS($M$). The first $M$ spins were stored in the first bit of each of these $M$ integers, the next $M$ spins in their second bit, and so forth. In other words, the $N_B$ bits of the integer IS($i$) contained the spins at sites $i$, $i + M$, $i + 2M$,..., $i + (N_B - 1)M$. Similarly, the next row of the lattice was held in the $M$ integers IS($M + 1$) to IS($2M$). In fact, in order to realize the periodic boundary conditions in

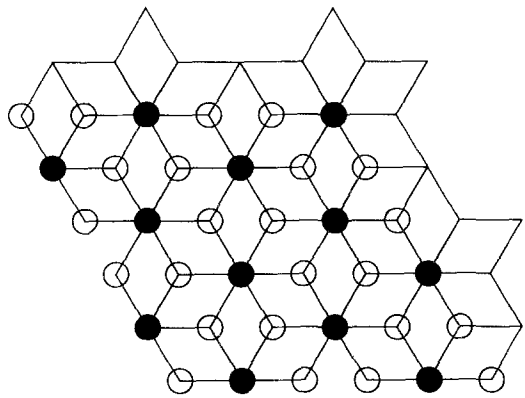

Fig. 5. Initial spin configuration corresponding to a flat surface with average orientation along the (111) direction (normal to the figure).

the up-down direction, the first $M$ integers of the array IS were used as a shadow row at the top of the lattice, IS$(M+1)$ through IS$((L+1)M)$ contained the $L$ rows of the actual lattice, and a final row of $M$ integers IS$((L+1)M+1)$ to IS$((L+2)M)$ shadowed the first row of the actual lattice.

Except for the "leftmost" sites [belonging to the integers IS$(M+1)$, IS$(2M+1)$,...] and the "rightmost" sites [belonging to IS$(2M)$, IS$(3M)$,...] the six nearest neighbors of a site stored in the $b$th bit of the integer IS$(i)$ will be found in the same ($b$th) bit of the integers IS$(i-1)$, IS$(i-M)$, IS$(i-M+1)$, IS$(i+1)$, IS$(i+M)$, and IS$(i+M-1)$ as depicted in Fig. 6.

For the exceptional sites in the "leftmost" words $M+1$, $2M+1$,... an exceptional loop is additionally required, since to obtain the correct neighbors on the left, in place of the integers IS$(i-1)$ and IS$(i+M-1)$, we must instead use the integers IS$(i-1+M)$ and IS$(i+2M-1)$, but subjected to a shift to the left by one bit. This shift also automatically accounts for the left–right periodic boundary conditions of the whole lattice.

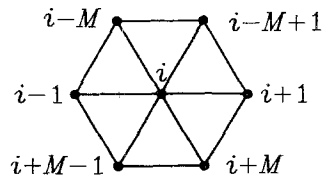


Fig. 6. Apart from the exceptional "leftmost" and "rightmost" words, the six nearest neighbors of a site stored in the $b$th bit of word $i$ will be found in the same $b$th bit of each of the words shown.

Similarly, we need an exceptional loop for the sites residing in the "rightmost" integers at $2M$, $3M$,.... The Fortran code for sweeping through the lattice with growth is described below. NSUBS is the number of sublattices, each of which is stored in NSITES words. ISUB labels the currently active sublattice and the array INDEX(ISUB, J) is used for stepping through each Jth word of the ISUBth sublattice. The updated lattice variables are held in the array ISNEW.

```
      DO 100 ISUB = 1, NSUBS
      IF (M.LT.3) GOTO 101
      DO 110 J = 1, NSITES
      I = INDEX (ISUB, J)
      IGRW = AND (EQV(IS(I), IS(I - 1)), AND (EQV(IS(I - 1),
                  IS(I + 1 - M)),
                  EQV(IS(I + 1 - M), IS(I + M))))
      NRNDS = NRNDS + 1
110   ISNEW(J) = XOR(IS(I), AND (IGRW, RG(NRNDS)))
101   CONTINUE
      :
```

The growth probability of $p^+$ is achieved by ensuring that in each element of the array RG, the bits are set with probability $p^+$. We chose $p^+ = 0.5$, as this is very easily and efficiently realized: each RG($i$) is simply set to a random integer in the range $-2^{(n-1)}$ to $2^{(n-1)} - 1$ inclusively, where $n$-bit integers are employed, implying that each bit of the integer is set independently with probability 1/2. Thus, assuming $N_B = 64$, one random number generation immediately delivers 64 bits set with probability $p^+ = 1/2$, whereas setting each bit separately would require 64 random number generations. In Table I we compare our results with this much slower procedure whereby the bits of each RG($i$) are set individually using separate random number generations. It can clearly be seen that both sets of results are statistically indistinguishable, confirming the validity of our procedure.

Other values of $p^+$ require more than one random integer generation: e.g., if I1 and I2 are two such randomly generated integers, then the bits in the integer I3 = AND(I1, I2) will be set with probability 1/4, while I4 = OR(I1, I2) has bits set with probability 3/4. In general, to obtain $p^+ = k/2^m$, for any odd $k$ between 1 and $2^m - 1$, where $m$ and $k$ are integers, $m$ random integers must be combined.

Line 110 then achieves the growth at a rate $p^+ = 1/2$ of the $N_B$ sites stored in the Ith integer, by flipping the appropriate bits if growth is

**Table I. Surface Width Data at $p^+ = p = 1/2$ for $L = 60$ and $L = 120$ Using Two Different Random Number Generation Schemes[a]**

| | $L = 60$ | | $L = 120$ | |
|---|---|---|---|---|
| $t$ | $w_a^2$ | $w_b^2$ | $w_a^2$ | $w_b^2$ |
| 1 | 1.279(3) | 1.277(3) | 1.281(2) | 1.279(3) |
| 2 | 1.313(4) | 1.309(4) | 1.312(3) | 1.315(3) |
| 4 | 1.424(7) | 1.423(6) | 1.426(5) | 1.431(6) |
| 8 | 1.57(1) | 1.566(9) | 1.570(9) | 1.576(7) |
| 16 | 1.72(1) | 1.71(1) | 1.72(1) | 1.72(1) |
| 32 | 1.88(2) | 1.86(2) | 1.88(2) | 1.88(2) |
| 64 | 2.00(3) | 2.00(2) | 2.01(2) | 2.04(2) |
| 128 | 2.11(3) | 2.11(3) | 2.17(3) | 2.16(3) |
| 256 | 2.20(4) | 2.20(4) | 2.27(4) | 2.32(4) |
| 512 | 2.20(4) | 2.17(4) | 2.38(5) | 2.44(5) |
| 1024 | 2.20(4) | 2.23(4) | 2.51(7) | 2.48(7) |

[a] The data $w_n^2$ were obtained by the method described in the text, where all of the $n$ bits of a word are set with probability 1/2 by setting the word to be a random integer uniformly distributed in the range $-2^{(n-1)}$ to $2^{(n-1)}-1$ inclusively. The data $w_b^2$ are from the much slower procedure of setting each bit of every word with probability 1/2 using separate random number generations. The number of independent runs was 150 for $L = 60$ and 50 for $L = 120$.

possible (i.e., if the appropriate bit of IGRW is TRUE) and if it is allowed by the random number mask RG.

The main loop (100) continues with the two exceptional loops. Analogously to the updating loop 110, the number of exceptional leftmost words is given by NEXL, INDXL is used for stepping through the active sublattice words, and ISNEWL holds the updated variables.

```
      :
C---EXCEPTIONAL LEFTMOST WORDS---
      DO 120 J = 1, NEXL
      I = INDXL(ISUB, J)
      ITEMP = CSMG(SHIFTR(IS(I - 1 + M), NB - 1),
                   SHIFTL(IS(I - 1 + M), 1), 1)
      IGRW = AND(EQV(IS(I), ITEMP), AND(EQV(ITEMP,
                 IS(I + 1 - M)),
                 EQV(IS(I + 1 - M), IS(I + M)))
      NRNDS = NRNDS + 1
120 ISNEWL(J) = XOR(IS(I), AND(IGRW, RG(NRNDS)))
```

The CSMG (Cray Scalar MerGe) achieves the desired shift (a cyclic shift with respect to the first $N_B$ bits of the integer). Note that $w = \text{CSMG}(x, y, z)$ assigns $w = x$, where $z$ has bits set (one) and $w = y$, where $z$ has bits reset (zero). This can be expressed in logical operations as $w = \text{OR}\{\text{AND}(x, z), \text{AND}(y, \text{NOT } z)\}$. If $N_B$ is equal to the number of bits in the computer word, then this merge can be replaced by a simple cyclic shift with respect to the whole word.

The loop for the exceptional rightmost words is similar, the updated variables are stored in ISNEWR, and the required shift is given by

```
ITEMP = CSMG(SHIFTL(IS(I − M2 + 1), NB − 1),
             SHIFTR(IS(I − M2 + 1), MSK)
```

where MSK is an integer with only the $N_B$th bit being set and M2 = 2M.

If evaporation is also to be included, it must be carried out next, before setting IS = ISNEW at the appropriate sites of the active sublattice ISUB. The loops for evaporating the sites with probability $p^-$ are very similar to the above. There a random number array RE must have each of its bits set with probability $p^-$ and an evaporation flag IEVP is calculated in an analogous fashion:

```
⋮
    IEVP = AND(EQV(IS(I), IS(I − M)), AND(EQV(S(I − M),
           S(I + 1)),
           EQV(IS(I + 1), IS(I − 1 + M))))
    NERNDS = NERNDS + 1
    IEVP = AND(IEVP, RE(NERNDS))
    ISNEW(J) = CSMG(XOR(S(I), IEVP), ISNEW(J), IEVP)
⋮
```

We similarly require two exceptional loops to take care of the sites residing in the exceptional rightmost and leftmost integers. Then the sites of the active sublattice are refreshed using ISNEW:

```
⋮
    DO 200 I = 1, NSITES
200 IS(INDEX(ISUB, I)) = ISNEW(I)
    DO 210 I = 1, NEXL
210 IS(INDXL(ISUB, I)) = ISNEWL(I)
    DO 220 I = 1, NEXR
220 IS(INDXR(ISUB, I)) = ISNEWR(I)
C---TAKE CARE OF UP-DOWN BOUNDARY CONDITIONS---
C   (LM = L * M)
```

```
CDIR$ IVDEP
      DO 300 I = 1, M
      IS(I + M + LM) = IS(I + M)
300   IS(I) = IS(I + LM)
100   CONTINUE
```

(The CDIR$ command is a compiler directive, which informs the compiler that the vector dependence following in loop 300 is to be ignored.)

The above updating loops fully vectorize and for the pure deposition case, $p^+ = 1/2$, $p^- = 0$, speeds of over 330 million updates per second were achieved for $L > 1000$ on one Cray X-MP/416 processor, including all the necessary random number generations each sweep. For the largest system that we simulated, $L = 11520$, over 2.76 million 64-bit words were required for the storage of the lattice variables IS, ISNEW, ISNEWL, and ISNEWR alone and each run consisting of 4096 complete sweeps of the lattice only took approximately 30 min of processor time.

## 4. THE MODEL IN HIGHER DIMENSIONS

The model presented above can in fact be generalized to higher dimensions. If $\hat{\mathbf{e}}_\alpha$ ($\alpha = 1, 2, \ldots, d+1$) are the $d+1$ unit vectors of a $(d+1)$-dimensional hypercubic crystal lattice, then when we project onto a $d$-dimensional surface lying normal to the (11...1) direction, we obtain $d+1$ projected vectors $\hat{\mathbf{e}}_\alpha^{\parallel}$ ($\alpha = 1, 2, \ldots, d+1$). These vectors are, of course, linearly dependent and satisfy $\sum_{\alpha=1}^{d+1} \hat{\mathbf{e}}_\alpha^{\parallel} = \mathbf{0}$. The projected $d$-dimensional lattice can be defined by using $d$ of the $\hat{\mathbf{e}}_\alpha^{\parallel}$ as basis vectors. A point $\mathbf{R} = \sum_{\alpha=1}^{d+1} n_\alpha \hat{\mathbf{e}}_\alpha$ on the surface has projection $\mathbf{x} = \sum_{\alpha=1}^{d+1} n_\alpha \hat{\mathbf{e}}_\alpha^{\parallel}$ on the $d$-dimensional lattice and has height

$$h(\mathbf{x}) = \sum_{\alpha=1}^{d+1} n_\alpha \tag{5}$$

above the (11...1) substrate plane.

Once again, due to the SOS restriction along the (11...1) direction on the growth of the original surface, there is a one-to-one mapping of points on the surface to points on the projected lattice, and, as before, two neighboring sites were either connected on the original surface, in which case their relative height difference is $\Delta h = \pm 1$, or they were not, implying $\Delta h = \mp d$. Hence, once more we may denote these two possibilities by connecting the sites by a satisfied (antiferromagnetic) bond if $|\Delta h| = 1$ and by a frustrated bond otherwise.

Now around any elementary plaquette of the lattice (see Fig. 7) there can be no net height change, implying the existence of one satisfied bond

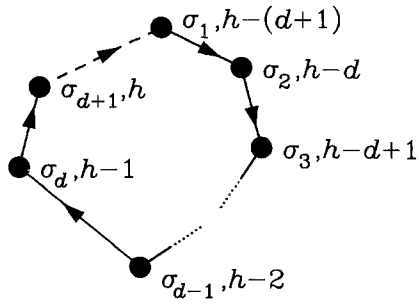


Fig. 7. An elementary plaquette of the $d$-dimensional substrate lattice is formed by taking each of the projected vectors $\hat{\mathbf{e}}_\alpha^{\parallel}$ tail-to-tail. Every such loop must contain precisely one frustrated bond (the dashed line) and $d$ satisfied bonds (the heavy lines). Each of the $d+1$ sublattices is visited once on traversing the loop. The height of a site on the $s$th sublattice is $n(d+1)+s$ for some integer $n$. Here $\sigma_j = \sigma_1 + j - 1 \pmod d$ for each $j = 1, \ldots, d+1$.

$\Delta h = -d$ (assuming we traverse the plaquette in the direction of the $\hat{\mathbf{e}}_\alpha^{\parallel}$), and $d$ frustrated bonds, $\Delta h = 1$. Such a configuration could not be realized by two-state Potts variables residing on the lattice vertices (unlike the $d=2$ case above): instead, these must also be generalized to (chiral) $d$-state Potts variables $\sigma(\mathbf{x}_i) \in \{0, 1, 2, \ldots, d-1\}$ with $\sigma(\mathbf{x}_i) = \sigma(\mathbf{x}_i + \hat{\mathbf{e}}_\alpha^{\parallel}) - 1 \pmod d$, signifying a satisfied bond between sites $\mathbf{x}_i$ and $\mathbf{x}_i + \hat{\mathbf{e}}_\alpha^{\parallel}$, and $\sigma(\mathbf{x}_i) \neq \sigma(\mathbf{x}_i + \hat{\mathbf{e}}_\alpha^{\parallel}) - 1 \pmod d$ a frustrated one. Then the relation (3) generalizes to

$$\Delta h \equiv h(\mathbf{x}_i + \hat{\mathbf{e}}_\alpha^{\parallel}) - h(\mathbf{x}_i) = 1 - (d+1)\,\delta\{\sigma(\mathbf{x}_i), \sigma(\mathbf{x}_i + \hat{\mathbf{e}}_\alpha^{\parallel})\} \tag{6}$$

with the Potts variables being assigned by

$$\sigma(\mathbf{x}_i) = h(\mathbf{x}_i) \bmod d \tag{7}$$

As before, $\Delta h = 1$ must imply $\sigma(\mathbf{x}_i) \neq \sigma(\mathbf{x}_i + \hat{\mathbf{e}}_\alpha^{\parallel})$, while if $\Delta h = -d$, then $\sigma(\mathbf{x}_i) = \sigma(\mathbf{x}_i + \hat{\mathbf{e}}_\alpha^{\parallel})$, showing the consistency of (6) and (7).

We saw above that any $2D$ surface configuration, when projected onto the substrate lattice corresponded to a ground state of the 2D triangular antiferromagnet. In general, any surface configuration of the $(d+1)$-dimensional model when projected onto the $d$-dimensional (11...1) substrate plane and represented by the mapping (7) will be a ground state of a chiral Potts model whose Hamiltonian is given by

$$H = -\sum_{\mathbf{x},\alpha} \delta\{\sigma(\mathbf{x}) + 1, \sigma(\mathbf{x} + \hat{\mathbf{e}}_\alpha^{\parallel})\} \tag{8}$$

where $\delta\{i, j\} = 1$ if $i = j \pmod d$, and 0 otherwise.

A particular feature of the mapping (7) is that the Potts variables on two neighboring sites connected by a frustrated bond (a height difference

of $d$ across) are actually identical. Thus, for any site $\mathbf{x}_i$ and its *principal* neighbor $\mathbf{x}_j = \mathbf{x}_i + \hat{\mathbf{e}}_\alpha^{\parallel}$ we have either $\sigma(\mathbf{x}_i) = \sigma(\mathbf{x}_j)$ or $\sigma(\mathbf{x}_i) = \sigma(\mathbf{x}_j) - 1 \pmod{d}$. That this is also a property of ground-state configurations of the chiral Potts model defined by (8) can be seen with the help of Fig. 7. Represented in the figure is an elementary plaquette of the $d$-dimensional substrate lattice, which is formed by adding the $d+1$ projected principal vectors $\hat{\mathbf{e}}_\alpha^{\parallel}$ tail to tail. Assume, without loss of generality, that the one frustrated bond of this loop occurs between the sites denoted by $\sigma_{d+1}$ and $\sigma_1$. Then across all other bonds we must have $\sigma_{j+1} = \sigma_j + 1 \pmod{d}$, $j = 1, 2, \ldots, d+1$. In particular, $\sigma_{d+1} = \sigma_1 + d \pmod{d} = \sigma_1$. In the following discussion we shall always restrict ourselves to the ground-state configurations of the chiral Potts model (8), and hence assume $\sigma_i = \sigma_j$ for the frustrated bonds.

As with the $d = 2$ case, a site may only grow if its height is less than that of all of the neighboring sites to which it is connected (i.e., to which it has a satisfied bond). This can only hold if it has satisfied bonds with each of its $d+1$ principal neighbors (giving a height decrease of 1) and has frustrated bonds with each of its $d+1$ nonprincipal neighbors (a height decrease of $d$). In other words, the Potts variables at that site must be the *same* as each of the *nonprincipal* neighbors and *one less* (mod $d$) than those of the *principal* neighbors. It is again sufficient to check only the former of these two requirements, for the following reason. If we already have frustrated bonds between the site in question and each of the $d+1$ nonprincipal neighbors, then for each such neighbor we can form an elementary plaquette which returns to the central site through a principal neighbor. As we already have a frustrated bond in this loop, the other $d$ bonds must be satisfied, which includes the bond between the central site and the principal neighbor through which we have returned. By symmetry, the argument applies to all $d+1$ principal neighbors. Consequently, there must be satisfied bonds between the site and each of its principal neighbors.

The deposition process of rate $p^+$ then consists in increasing the height of an eligible site by $d+1$, which, in terms of the Potts variables, consists in changing $\sigma \to \sigma + 1 \pmod{d}$. Evaporation at rate $p^-$ consists in checking whether $\sigma$ at the given site is identical to those of the four principal neighbors and, if so, $\sigma \to \sigma - 1 \pmod{d}$ with probability $p^-$. This results in a height decrease at the site by an amount $d+1$.

Just as for the $d = 2$ case, the whole $(d+1)$-dimensional crystal may be viewed as a stack of $(d+1)$-dimensional hypercubes on the (11...1) substrate hyperplane and the SOS restriction along the (11...1) direction is equivalent to demanding that at most $(d+1)$ of the $2(d+1)$ faces of each hypercube may be exposed (i.e., may be part of the surface). A stacking event consists in adding a hypercube to the stack at a rate $p^+$ (deposition)

or removing a hypercube at a rate $p^-$ (evaporation). This must maintain the SOS condition, which implies that the number of exposed ($d$-dimensional) faces must be conserved, whence the addition of a hypercube is only allowed when $d+1$ of its faces make direct contact with exposed faces in the stack. Similarly, a hypercube may only be removed if it has precisely $d+1$ exposed faces.

The natural underlying structure of three sublattices which we pointed out in the $d=2$ case also generalizes to $d+1$ sublattices in $d$ dimensions. The sublattices are revealed by noting that we may cover the lattice with elementary plaquettes. Then on each plaquette we have one site belonging to each of the $d+1$ sublattices and the $2(d+1)$ nearest neighbors of a particular site belong to different sublattices from that of the site. Furthermore, the $d+1$ principal neighbors all belong to a common sublattice and the $d+1$ nonprincipal ones all belong to another. Each such plaquette consists of one frustrated and $d$ satisfied bonds.

Consider once more the representative elementary plaquette shown in Fig. 7 and assume that the site denoted by $\sigma_{d+1}$ has a height $h$. Then across the frustrated bond the site denoted by $\sigma_1$ will have a height $h-(d+1)$. Continuing around the elementary plaquette, only satisfied bonds remain, so the heights of the other sites are $h-d$, $h-d+1$,..., $h-1$. We then have that on each $s$th sublattice the heights take the form $h_i^{(s)} = n(d+1)+s$ for some integer $n$.

We now proceed to describe the particular case of $d=3$, which we also have simulated. There the four unit vectors of the 4D hypercubic lattice are mapped onto 4 vectors forming a tetrahedron in 3D, thus giving rise to a body-centered cubic (BCC) lattice (see Fig. 8a). For the simulation we

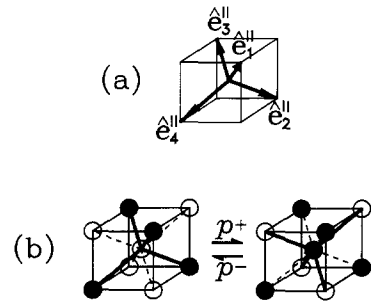


Fig. 8. (a) The four projected unit vectors $\hat{\mathbf{e}}_\alpha^{\parallel}$ of the 4D hypercubic lattice. The projected 3D substrate lattice is revealed by taking 3 of these vectors as basis vectors, producing a body-centered cubic (BCC) lattice. (b) The local updating rule on the BCC substrate lattice for deposition (left to right at rate $p^+$) and evaporation (right to left at rate $p^-$). The cubes shown here serve only as a guide to the eye.

employed two sublattices, corresponding to the two interpenetrating simple-cubic (SC) lattices of which a BCC lattice is composed. Thus, each of our simulation sublattices contained two of the sublattices elucidated above. The deposition ($p^+$) and evaporation ($p^-$) processes are shown in Fig. 8b.

One-bit-per-site multisite coding was, of course, not possible in this case—we had instead to use two bits per site, since we were dealing with 3-state Potts variables. We do not describe in detail the Fortran code for this case, but only point out the main features.

The two interpenetrating SC lattices of size $L \times L \times L$—labeled A and B, with A being half a layer above B—were stored in separate pairs of arrays: the A lattice in AR and AL and the B lattice in BR and BL. Here L and R denote respectively the left and right bits of the binary representation of the Potts variables. That is, the two bits representing each $\sigma$ residing on lattice A (resp. B) were accommodated in the same (say) $b$th bit of AL($i$) and AR($i$) [resp. BL($i$) and BR($i$)] for some element $i$. Then, apart from this need to use two bits for each $\sigma$, the multisite coding followed in spirit that of the $d=2$ case: each $L \times L$ layer of each SC sublattice was accommodated in a total of $L+1$ rows of $M = L/N_B$ pairs of integers, an additional top (resp. bottom) row being required in each layer to invoke the periodic up–down boundary conditions on the A (resp. B) sublattice. In addition, to fulfill the boundary conditions between the uppermost A layer and the lowermost B layer, the A sublattice required an additional shadow layer on the bottom and the B sublattice an additional shadow layer on the top. Thus, in all, each sublattice was stored in a total of $2(L+1)^2 M$ integers. For each update, any site of sublattice A only referred to sites of B and vice versa. Hence, the loops over all the sites in a given sublattice could be vectorized. As before, additional loops (one for each sublattice) were also needed to take account of the exceptional words.

The necessary bit operations at the heart of the growth and evaporation processes should be clear from Table II: for a site which can grow, the new left and right bits will be respectively L′ = R and R′ = EQV(L, R), where EQV is the bitwise logical equivalence operation. Specifically, if the word IGRW has each bit set according to whether the corresponding sites are eligible for growth (including the growth probability $p^+$), then a growth update on all the sites in the Ith pair of words of sublattice A is achieved simply by

```
ARNEW(I) = CSMG(EQV(AR(I), AL(I)), AR(I), IGRW)
ALNEW(I) = CSMG(AR(I), AL(I), IGRW)
```

and similarly for sublattice B. For evaporation, the updating procedure is L″ = EQV(L, R) and R″ = L.

**Table II. Binary Representation Used in Multisite-Coding Implementation of the $d=3$ Model[a]**

| Potts variable | Binary representation | | After growth | | | After evaporation | | |
|---|---|---|---|---|---|---|---|---|
| $\sigma_A$ | AL | AR | $\sigma'_A$ | AL′ | AR′ | $\sigma''_A$ | AL″ | AR″ |
| 0 | 0 | 0 | 1 | 0 | 1 | 2 | 1 | 0 |
| 1 | 0 | 1 | 2 | 1 | 0 | 0 | 0 | 0 |
| 2 | 1 | 0 | 0 | 0 | 0 | 1 | 0 | 1 |

[a] L and R denote, respectively, the left and right bits of the Potts variable $\sigma=0$, 1, and 2.

As in the $d=2$ case, the updating loops fully vectorized. For $L=256$, a rate of over 130 million updates per second per Cray X-MP/416 processor was achieved for the pure deposition case, $p^+=1/2$, $p^-=0$, while the equilibrium case, $p^+=p^-=1/2$, reached 72 million updates per second.

## 5. TEST OF THE ALGORITHM

We have applied the above algorithm to systems of up to $N=L^2=11520^2$ sites in the $d=2$ case and $N=2L^3=2\times 192^3$ sites in the $d=3$ case to determine the roughness exponents and to investigate possible nonequilibrium roughening transitions. Details of this study will be reported elsewhere.[12] By setting $p^+=p^-$, the model describes a local kinetic rule for the time evolution of a stationary (nongrowing) surface. An exact expression for the height–height correlation function in the two-dimensional equilibrium case of the model was derived by Blöte and Hilhorst.[13] It seems to be worthwhile to test our algorithm and the implementation of it against this known result. This will be the topic of the remaining part of the paper.

The exact result of Blöte and Hilhorst[13] indicates that the two-dimensional equilibrium surface is logarithmically rough due to thermal fluctuations, with a stiffness constant $K=2\pi/9$. The equilibrium width of a surface of linear size $L$ is then given by

$$w_{\text{eq}}^2=\frac{1}{\pi K}\ln L+\text{const} \tag{9}$$

Assuming that the steady-state distribution of our growth model at

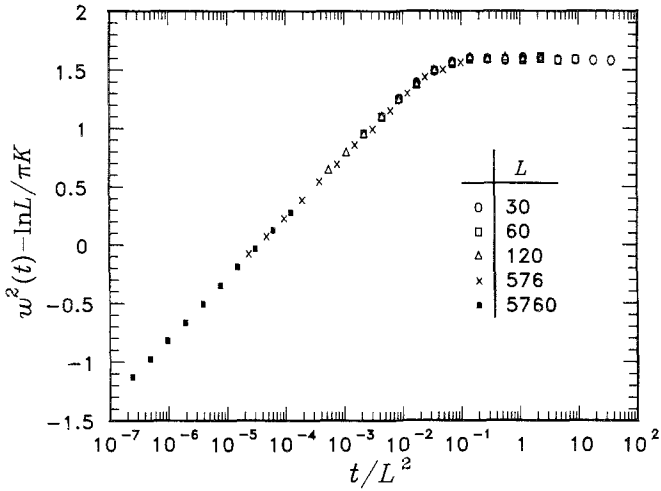


Fig. 9. Scaling plot of mean-square surface width $w^2$ at $p^+ = p^- = 1/2$ as a function of time $t$ for various system sizes $L$. All data collapse onto a common line, in agreement with the scaling form (10).

$p^- = p^-$ is the same as the infinite-temperature surface model,[4] we find that the equilibrium surface width in our model should have the same size dependence (6). In addition, we may expect a dynamical exponent $z = 2$ as in the theory of Edwards and Wilkinson[16] for surface growth models which are described by a *linear* Langevin equation.[5] Based on (9) and the observation that, starting from a flat surface at $t = 0$, the surface width at $t \ll L^2$ is independent of $L$, we may plausibly write

$$w_2(t) = (1/\pi K) \ln[L\tilde{f}(t/L^2)] \tag{10}$$

where $\tilde{f}(x) \sim x^{1/2}$ for $x \ll 1$ and goes to a constant as $x \to \infty$. Thus, for $t \ll L^2$ we expect $w^2(t) \simeq (1/2\pi K) \ln t + \text{const}$.

Figure 9 shows our Monte Carlo data at $p^+ = p^- = 1/2$ for five different sizes $L = 30$, 60, 120, 576, and 5760 at $t = 2^k$, $k \geqslant 3$. The exact value $K = 2\pi/9$ is used in making the scaling plot. Error bars on the data are much smaller than the plotting symbols. The data collapse is in excellent agreement with Eq. (10).

[4] One can show that an algorithm based on random selection of sublattices for updating satisfies the detailed balance condition. The sequential updating scheme adopted here may not fulfill this condition. Nevertheless, it may still generate the same steady-state distribution as in the first case.

[5] The absence of a nonlinear term in the Langevin equation for the equilibrium surface has been argued by Plischke *et al.*[6]

## ACKNOWLEDGMENTS

We are indebted to D. E. Wolf for many helpful discussions and suggestions. We are also very grateful to D. Stauffer for his many useful comments on the manuscript.

## REFERENCES

1. T. A. Witten and L. M. Sander, *Phys. Rev. Lett.* **47**:1400 (1981).
2. M. Eden, in *Symposium on Information Theory in Biology*, H. P. Yockey, ed. (Pergamon Press, New York, 1958), p. 359.
3. F. Family and T. Vicsek, *J. Phys. A* **18**:L75 (1985).
4. M. Plischke and Z. Rácz, *Phys. Rev. A* **32**:3825 (1985).
5. P. Meakin, P. Ramanlal, L. M. Sander, and R. C. Ball, *Phys. Rev. A* **34**:5091 (1986).
6. M. Plischke, Z. Rácz, and D. Liu, *Phys. Rev. B* **35**:3485 (1987); D. Liu and M. Plischke, *Phys. Rev. B* **38**:4781 (1988).
7. R. Jullien and R. Botet, *J. Phys. A* **18**:2279 (1985).
8. M. Kardar, G. Parisi, and Y.-C. Zhang, *Phys. Rev. Lett.* **56**:889 (1986).
9. J. G. Zabolitzky and D. Stauffer, *Phys. Rev. A* **34**:1523 (1986); *Phys. Rev. Lett.* **57**:1809 (1986).
10. D. E. Wolf and J. Kertész, *Europhys. Lett.* **4**:561 (1987); J. Kertész and D. E. Wolf, *J. Phys. A* **21**:747 (1988); D. E. Wolf, in *Kinetics of Ordering and Growth at Surfaces*, M. Lagally, ed. (Plenum, New York, 1989).
11. P. Devillard and H. E. Stanley, *Phys. Rev. A* **38**:6451 (1988).
12. B. M. Forrest and L.-H. Tang, *Phys. Rev. Lett.* **64**:1405 (1990); L.-H. Tang, B. M. Forrest, and T. Nattermann, in preparation.
13. H. W. J. Blöte and H. J. Hilhorst, *J. Phys. A* **15**:L631 (1982).
14. J. M. Kim and J. M. Kosterlitz, *Phys. Rev. Lett.* **62**:2289 (1989).
15. R. Zorn, H. J. Herrmann, and C. Rebbi, *Comput. Phys. Commun.* **23**:337 (1981); C. Kalle and V. Winkelmann, *J. Stat. Phys.* **28**:639 (1982); S. Wansleben, J. G. Zabolitzky, and C. Kalle, *J. Stat. Phys.* **37**:271 (1984); G. O. Williams and M. H. Kalos, *J. Stat. Phys.* **37**:283 (1984); H. J. Herrmann, *J. Stat. Phys.* **45**:145 (1986).
16. S. F. Edwards and D. R. Wilkinson, *Proc. R. Soc. Lond. A* **381**:17 (1982).